VIII International Conference on Computational Methods in Marine Engineering
MARINE 2019
R. Bensow and J. Ringsberg (Eds)

SIMULATION OF IRREGULAR WAVE MOTION USING A FLAP-TYPE WAVEMAKER

S. RAMEZANZADEH [1, †], M. OZBULUT [2] AND M. YILDIZ [1, †]

[1] Faculty of Engineering and Natural Sciences, Sabanci University, Istanbul 34956, Turkey
Email: ramezanzadeh@sabanciuniv.edu - Web page: http://www.sabanciuniv.edu

[2] Faculty of Engineering, Piri Reis University, Istanbul 34940, Turkey
Email: mozbulut@pirireis.edu - Web page: http://www.pirireis.edu.tr

[†] Integrated Manufacturing Technologies Research and Application Center, Sabanci University, Tuzla, Istanbul 34956, Turkey

Keywords: SPH Method, Numerical Wave Tank, Irregular Wave, Wave Energy Spectrum

Abstract. The main objective of the present study is to propose a numerical scheme to model irregular wave systems through a Lagrangian, particle-based numerical method, namely, Smoothed Particle Hydrodynamics (SPH). A numerical wave generator tank, which can generate desired irregular waves is modeled by the SPH method. The fluid motion is governed by continuity and Navier-Stokes equations where Weakly Compressible SPH (WCSPH) approximation is employed for the numerical discretization of the problem domain. To generate the irregular wave spectrum, a flap-type wave generator is adopted into the computational domain which yields to the modeling of moving boundary conditions on the problem domain. As benchmark studies, JONSWAP and Pierson-Moskowitz wave spectrums are simulated to validate the obtained wave characteristics with the theoretical results. The performances of the wave maker are tested under different peak wave frequency values. Fast Fourier Transformation (FFT) analysis is conducted to scrutinize the distribution of wave energy spectrum in the frequency domain. In the light of sufficiently long-term simulation results, it can be said that a good agreement is obtained between the numerical and theoretical results, which indicates that the presented SPH scheme can be utilized in further free-surface hydrodynamics studies related to the irregular wave regimes.

1 INTRODUCTION

Ocean surface waves generally produce periodic pressure loads on floating or fixed marine structures; therefore, the problem of determining the motion of objects under the influence of oceanic waves and determining hydrodynamic forces on these objects is an area which gets a lot of interest among free-surface water scientists. Further research on wave mechanics is required in today's engineering applications, namely, marine sciences, coastal engineering, port management, the design of any offshore structures like ships, and wave energy systems.

Regular waves do not represent the real state of the sea because the nature of oceanic waves is mostly random or irregular. Indeed, these waves can be considered as the summation of many regular waves, each with its own amplitude, period or frequency, length, and propagation direction [1]. Fast Fourier transformation (FFT) can be used to transfer random sea surface into the summation of linear waves. A wave spectrum describes the distribution of wave energy over a frequency range for a given sea or ocean region [2]. There are several wave spectra available in the literature and JONSWAP and Pierson-Moskowitz which are modeled in this study are one of the most common irregular wave systems [2-4].

As a natural consequence of the development of new generation technology on experimental opportunities, today, scientific studies on the investigation of free-surface flows can get more realistic and accurate results. Numerous experimental researches have been carried out to investigate the spread of irregular waves and their interaction with the offshore structures [5-7]. On the other hand, although experimental studies capture and reveal the physical background of such problems in a more realistic way, they are generally an expensive tool for the specific industrial applications. Alternatively, compared to experimental testing, a relatively reliable and cheaper technique is the computational modeling and analysis of the wave conditions in a numerical wave tank.

Along this line, this work aims to utilize one of the popular computational technique on the modeling of free surface problems, a Lagrangian, particle-based method named as Smoothed Particle Hydrodynamics (SPH). The SPH method has been used in modeling of free-surface water flow problems since the mid-90s [8]. The application of the SPH method to study coastal engineering problems has increased during the last few years [9-13]. Due to its intrinsic advantages on the modeling of highly nonlinear violent free-surface problems, the SPH method has been widely used in numerical calculations to capture high free-surface deformations which may occur in the problem domain. The method defines the physical behavior of the fluid through an interpolation process using a weight function that varies in proportion to the position of the particles distributed within the problem area. The physical properties (density, pressure, velocity, etc.) of each particle are updated at each time step so that the time-varying physical properties of each particle can be tracked instantaneously.

In this study, a numerical wave tank which generates desired irregular waves is modeled. The fluid motion is governed by continuity and Navier-Stokes equations, and Weakly Compressible SPH (WCSPH) approximation is employed for the numerical discretization of the problem domain. To generate the irregular wave spectrum in a more realistic manner, a flap-type wave generator is adopted into the computational domain which yields to the modeling of moving boundary conditions on the problem domain.

The rest of the paper is organized as follows: In the second section, the governing equations and the discretization methodology of these equations together with the corrective treatments are stated. Following the mathematical background of the irregular wave systems utilized in this work, the physical parameters of the problem and obtained numerical results are presented in the third section. Finally, the concluding remarks are emphasized in the last part.

2 MATHEMATICAL FORMULATIONS

2.1 Governing equations

In the present study, the fluid is assumed to be weakly compressible. The continuity equation and Navier-Stokes equations are employed to describe the fluid motion and can be written as:

$$\frac{d\rho}{dt} = -\rho\nabla \cdot \vec{\boldsymbol{u}} \tag{1}$$

$$\frac{d\vec{\boldsymbol{u}}}{dt} = -\frac{1}{\rho}\nabla p + \upsilon\nabla^2\vec{\boldsymbol{u}} + \vec{\boldsymbol{g}} \tag{2}$$

The displacement of fluid particles is provided by the following equation:

$$\frac{d\vec{\boldsymbol{r}}}{dt} = \vec{\boldsymbol{u}} \tag{3}$$

Where $\vec{\boldsymbol{u}}$ is the velocity vector, p is the pressure, υ is the kinematic viscosity, ρ is the density, $\vec{\boldsymbol{r}}$ is the particle positions and $\vec{\boldsymbol{g}}$ denotes gravitational acceleration vector. The governing equations are discretized utilizing WCSPH method [8]. In this approach, the pressure term is determined by the implementation of the artificial equation of state, which couples pressure and density variations through a coefficient commonly known as the speed of sound. In the present study, the equation of state proposed by Monaghan [14] is used:

$$p = \frac{\rho_0 c_0^2}{\gamma}\left[\left(\frac{\rho}{\rho_0}\right)^{\gamma} - 1\right] \tag{4}$$

Where c_0 is the reference speed of sound taken as 30 [m/s], ρ_0 is the reference density equal to 1000 [kg/m^3], and γ is the specific heat ratio of water (considered to be 7). The reference speed of sound is determined by dimensionless Mach number (M), which represents the ratio of fluid to sound velocities. The amount of M lower than 0.1 guarantees the density fluctuations less than the 1% of the reference density [14].

2.2 SPH scheme and numerical discretization of the governing equations

The SPH method is based on the interpolation process. According to this approach, any field function is expressed by means of the interaction of neighboring particles using an analytic function called the weight function. The weight function, $W(r_{ij},h)$, is defined as a function, equivalent to Delta Dirac (δ) when h, interpolation length, is zero. Mathematically, any continuous function (scalar, vectorial, or tensor) can be written as follows:

$$A(\vec{\boldsymbol{r}}_i) = \int_{\Omega} A(\vec{\boldsymbol{r}}_j)\delta(\vec{\boldsymbol{r}}_i - \vec{\boldsymbol{r}}_j)d^3\vec{\boldsymbol{r}}_{ij} \tag{5}$$

$$\int_{\Omega} \delta(\vec{\boldsymbol{r}}_i - \vec{\boldsymbol{r}}_j)d^3\vec{\boldsymbol{r}}_{ij} = \begin{cases} 1, & \vec{\boldsymbol{r}}_i = \vec{\boldsymbol{r}}_j \\ 0, & \vec{\boldsymbol{r}}_i \neq \vec{\boldsymbol{r}}_j \end{cases} \tag{6}$$

Where $A(\vec{\boldsymbol{r}}_i)$ is the continuous function, $\vec{\boldsymbol{r}}_{ij} = \vec{\boldsymbol{r}}_i - \vec{\boldsymbol{r}}_j$ represents the distance vector between the particle of interest i and its neighboring particle j, and $\vec{\boldsymbol{r}}_i$ and $\vec{\boldsymbol{r}}_j$ represents the position vectors for the i and j particles, respectively. Value of any continuous function, $A(\vec{\boldsymbol{r}}_i)$, is expressed in the SPH method as follows:

$$A_i \cong \langle A(\vec{\boldsymbol{r}}_i)\rangle \equiv \int_{\Omega} A(\vec{\boldsymbol{r}}_j)W(r_{ij},h)d^3\vec{\boldsymbol{r}}_{ij} \tag{7}$$

In the above formulation, the angle bracket $\langle\ \rangle$ defines the kernel approximation and $d^3\vec{\boldsymbol{r}}_{ij}$ denotes the infinitesimally small volume of the particle which equals to the mass, m_j, divided by the density of the particle, ρ_j, and Ω represents the total bounded volume of the domain. A_i function represents any hydrodynamic properties such as velocity, pressure, density, and viscosity. In the SPH method, the derivative of any arbitrary function can be easily calculated by taking the derivative from the weight function:

$$\langle\frac{\partial A(\vec{\boldsymbol{r}}_i)}{\partial x_i^k}\rangle \equiv -\int_{\Omega} A(\vec{\boldsymbol{r}}_j)\frac{\partial W(r_{ij},h)}{\partial x_i^k}d^3\vec{\boldsymbol{r}}_{ij} \tag{8}$$

There are various kinds of kernel functions in the literature [15, 16]. In this study, the quintic kernel function is utilized due to its high accuracy and stability [17]:

$$W(R,h) \quad = \alpha_d \begin{cases} (3-R)^5 - 6(2-R)^5 + 15(1-R)^5, & 0 \le R < 1 \\ (3-R)^5 - 6(2-R)^5, & 1 \le R < 2 \\ (3-R)^5, & 2 \le R < 3 \\ 0, & R \ge 3 \end{cases} \tag{9}$$

In Eq. (9), $R = |\vec{r}_{ij}|/h$, h is the smoothing length, and α_d is a coefficient dependent on the dimension of the problem. In two dimensions, α_d is equal to $7/(478\pi h^2)$. As a result, the numerical discretization of the the continuity and momentum equations of fluid motion can be expressed respectively by the following relations [14, 18]:

$$\frac{d\rho_i}{dt} = \rho_i \sum_{j=1}^{N} (\vec{\boldsymbol{u}}_i - \vec{\boldsymbol{u}}_j) \cdot \nabla_i W_{ij} V_j \tag{10}$$

$$\rho_i \frac{d\vec{\boldsymbol{u}}_i}{dt} = -\sum_{j=1}^{N} (\frac{p_i}{\rho_i^2} + \frac{p_j}{\rho_j^2}) \nabla_i W_{ij} V_j + K\nu \sum_{j=1}^{N} \Pi_{ij} \nabla_i W_{ij} V_j + \vec{\boldsymbol{g}} \tag{11}$$

Here, N is the number of neighbor particles for particle i, ∇_i is the gradient operator taken with respect to the position of particle i, $K=2(n+2)$ where n is the dimension of the problem domain, V_j indicates the volume of particles which is calculated by $V_j = \sum_{j=1}^{N} 1/W_{ij}$ and Π_{ij} is the viscosity term which is defined as [19]:

$$\Pi_{ij} = \frac{(\vec{\boldsymbol{u}}_j - \vec{\boldsymbol{u}}_i) \cdot (\vec{\boldsymbol{r}}_j - \vec{\boldsymbol{r}}_i)}{\|\vec{\boldsymbol{r}}_j - \vec{\boldsymbol{r}}_i\|^2} \tag{12}$$

Kinematic viscosity (υ) is taken as 10^{-6} (m^2/s) for water.

2.3 Corrective numerical algorithms

In this section, we will briefly mention the correction terms added into the numerical scheme to increase the stability and robustness of the method.

2.3.1 Kernel gradient correction

In this study, in order to increase the accuracy of the evaluation of any linear velocity field and conservation of angular momentum, the derivatives of the kernel function given by Eq. (9) is renormalized by multiplying with the following local $L(\vec{\boldsymbol{r}}_i)$ matrix [20, 21]:

$$\nabla^C W_{\vec{r}_i} = L(\vec{\boldsymbol{r}}_{\boldsymbol{i}})\nabla_{\boldsymbol{i}} W_{\boldsymbol{ij}} \tag{13}$$

$$L(\vec{\boldsymbol{r}}_{\boldsymbol{i}}) = \left[\sum_j \begin{pmatrix} x_{ji}\dfrac{\partial W_{\boldsymbol{ij}}}{\partial x_i} & y_{ji}\dfrac{\partial W_{\boldsymbol{ij}}}{\partial x_{\boldsymbol{i}}} \\ x_{ji}\dfrac{\partial W_{\boldsymbol{ij}}}{\partial y_{\boldsymbol{i}}} & y_{ji}\dfrac{\partial W_{\boldsymbol{ij}}}{\partial y_{\boldsymbol{i}}} \end{pmatrix} V_{\boldsymbol{j}}\right]^{-1} \tag{14}$$

2.3.2 Density correction

In the weakly compressible SPH approach, the precise calculation of the density field is crucial because the pressure values are coupled to the density values in the equation of state (see Eq. 4) and small density disturbances can lead to high oscillations in the pressure field, and in turn, cause a decline in numerical accuracy and stability [22]. In order to eliminate this problem, density correction algorithms are frequently used in SPH literature [19, 23]. In this study, The density correction algorithm is applied through:

$$\hat{\rho}_{\boldsymbol{i}} = \rho_{\boldsymbol{i}} - \frac{\sum_{j=1}^{N}(\rho_i - \rho_j)W_{ij}}{\sum_{j=1}^{N} W_{ij}} \tag{15}$$

Here, $\hat{\rho}_{\boldsymbol{i}}$ is the corrected density.

2.3.3 Hybrid free-surface and artificial particle displacement algorithm

Velocity variance-based free-surface algorithm (VFS) is a numerical correction treatment which is applied to only free-surface particles and help the particles on the free-surface to stay away from excessive scattering by providing a numerical surface tension on the free surface. The particles which have neighbor particle amount less than 65% of the average neighbor particle number in the problem domain are marked as free-surface articles along this line, the applied free-surface treatment is given below [22, 24]:

$$\delta\vec{\boldsymbol{u}}_{\boldsymbol{i}} = \frac{\sum_{j=1}^{N}(\vec{\boldsymbol{u}}_{\boldsymbol{i}} - \vec{\boldsymbol{u}}_{\boldsymbol{j}})W_{\boldsymbol{ij}}}{\sum_{j=1}^{N} W_{ij}}, \quad \hat{\vec{\boldsymbol{u}}}_{\boldsymbol{i}} = \vec{\boldsymbol{u}}_{\boldsymbol{i}} - \varepsilon\delta\vec{\boldsymbol{u}}_{\boldsymbol{i}} \tag{16}$$

where $\hat{\vec{\boldsymbol{u}}}_{\boldsymbol{i}}$ is the corrected particle velocity, and ε is a constant which is sufficient to assign a value between 0.05 and 0.1 times the initial particle spacing (*dx*). On the other hand, Artificial Particle Displacement (APD) algorithm which is applied to the fully populated regions of the fluid domain provides a homogeneous particle distribution during the evolution of the flow which significantly enhances the accuracy of the interpolation processes of the SPH method. The formulation of the APD algorithm is as follows [22, 24]:

$$\delta\vec{\boldsymbol{r}}_{\boldsymbol{i}} = \sum_{j=1}^{N} \frac{\vec{r}_{\boldsymbol{ij}}}{r_{\boldsymbol{ij}}^3} r_0^2 u_{cff} \Delta t \tag{17}$$

$$r_0 = \frac{1}{N}\sum_{j=1}^{N} r_{\boldsymbol{ij}} \ , \ u_{cff} = |\delta\vec{\boldsymbol{u}}_{\boldsymbol{i}}|$$

2.4 Irregular wave generation

The procedure for the generation of these irregular waves starts from dividing the wave density spectrum into *n* equal parts ($n > 50$) in a frequency domain which separates spectrum into *n* equal monochromatic waves each with their own wave characteristics like amplitude, frequency, and wavelength [25]. Angular frequencies and amplitudes of all wave components are calculated as follows:

$$\omega_i = 2\pi f_i \tag{18}$$

$$a_i = \sqrt{2S_\eta(f_i)\Delta f} = \frac{H_i}{2} \tag{19}$$

Where f_i indicates the frequency of each wave, H_i denotes the correponding wave heights, $S_\eta(f_i)$ represents the wave energy spectrum of each wave frequency, ω_i is the angular frequency, and a_i is the amplitude. The time series of wave amplitudes are converted into the flap movement by means of the Biesel transfer function [26] :

$$\frac{H_i}{S_{0,i}} = 4\left(\frac{sinh\, k_i d}{k_i d}\right)\frac{k_i d\ sinh\, k_i d - cosh\, k_i d + 1}{sinh\, 2k_i d + 2k_i d} \tag{20}$$

where d is the water depth, k_i is the wave number (calculated by $k_i = \omega_i^2/g$), and δ_i is the initial phase which is a random number between 0 and 2π. All wave components obtained by Eq. 20 are combined in the flap displacement time series equation:

$$e(t) = \sum_{i=1}^{n} \frac{S_{0,i}}{2} sin(\omega_i t + \delta_i) \tag{21}$$

The present study aims to model two standard wave spectra to generate irregular wave trains, namely, JONSWAP (Joint North Sea Wave Project) and Pierson-Moskowitz spectra.

2.4.1 JONSWAP wave spectrum

Various wave energy spectra are found in literature and used for ocean engineering problems [2], JONSWAP is one of the most common spectrum among them, which is an experimental relationship that describes the distribution of energy with a frequency in the ocean. JONSWAP was developed by Hasselmann from 1968 to 1969 [3] after analyzing and measuring data collected during the Joint North Sea Wave Study Project. The following equation of JONSWAP wave spectrum is recommended by the 23th ITTC in 2002 for limited fetch conditions [2]:

$$S(f) = \alpha g^2 (2\pi)^{-4} f^{-5}\, exp\left[-\frac{5}{4}\left(\frac{f}{f_P}\right)^{-4}\right] \gamma^{exp\left[-\frac{(f-f_P)^2}{2\tau^2 f_P^2}\right]} \tag{22}$$

$$\tau = 0.07 \quad , f \leq f_P$$
$$\tau = 0.09 \quad , f > f_P$$
$$\alpha = 0.0081$$

Where g is the gravity acceleration, f_P is the wave peak frequency in Hertz, and γ is the wave peak enhancement factor taken as 3.3.

2.4.2 Pierson-Moskowitz wave spectrum

The Pierson-Moskowitz spectrum is based on measurements taken in the North Atlantic Ocean [4]. This spectrum is proper for fully developed wind sea studies:

$$S(f) = \frac{A}{f^5} exp\left(-\frac{B}{f^4}\right) \tag{23}$$

$$A = \alpha g^2 (2\pi)^{-4}$$
$$B = (5/4) f_P^4$$

where A is the scaling parameter and α is the intensity of the spectrum that relates to the wind speed and fetch length. In this study, α is taken as 8.1×10^{-3}.

3 PROBLEM DEFINITION AND NUMERICAL RESULTS

3.1 Problem definition

The geometrical scheme of the two-dimensional numerical wave tank is shown in Fig.1. The flap-type wavemaker in the left-hand side of the tank generates the required irregular waves. The still water level and the channel horizontal length were taken d = 1 [m] and L = 5 [m], respectively. The initial interparticle distance equals to dx = 0.01 [m], which leads to the employment of 66,840 fluid particles in all of the simulations. In order to physically dampen the produced waves without using any numerical damping algorithm, a linearly increasing beach with an angle of β = 21.8° is placed at the end of the tank. The wave heights are recorded at x_{rec} = 2.5 [m] from the flap, and the obtained wave heights time series are compared with theoretical solutions.

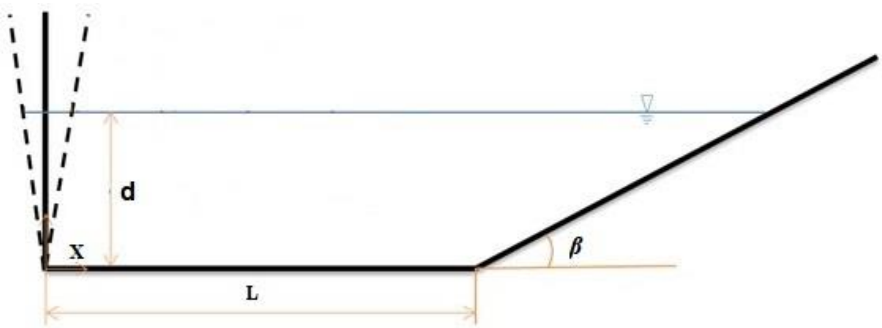

Figure 1: Numerical wave tank setup

3.2 Numerical results

Irregular wave simulations of two different wave spectra and three peak frequencies for each spectrum are performed with the SPH solution scheme described in Chapter 2. The summary of the simulation cases in the present study is provided in Table 1.

Table 1: Spectrum type, frequency range and peak frequencies of the simulated test cases

Case No	Spectrum Type	Frequency Range	Peak Frequency
1	JONSWAP	0.3-2.5 Hz	0.6 Hz
2	JONSWAP	0.3-2.5 Hz	0.7 Hz
3	JONSWAP	0.5-2.5 Hz	0.8 Hz
4	Pierson-Moskowitz	0.3-3.0 Hz	0.6 Hz
5	Pierson-Moskowitz	0.3-3.0 Hz	0.7 Hz
6	Pierson-Moskowitz	0.3-3.0 Hz	0.8 Hz

Fig.2 and Fig.3 depict the time series of both wave spectrum types obtained by calculated wave elevations from still water level at point $x = x_{rec}$. It can be said that the obtained SPH results are consistent with the theoretical wave height of the irregular waves especially while the peak frequency value is increasing in both wave spectra. The main reason for the discrepancies between the obtained free surface elevations and the theoretical solution can be attributed to the presence of the relatively low number of wave components which have higher wavelengths causing reflection from the damping beach at the end of the tank. To overcome this physical problem, a longer wave tank is required which leads to the utilization of a higher amount of particles hence causing a dramatical increase in terms of computational costs.

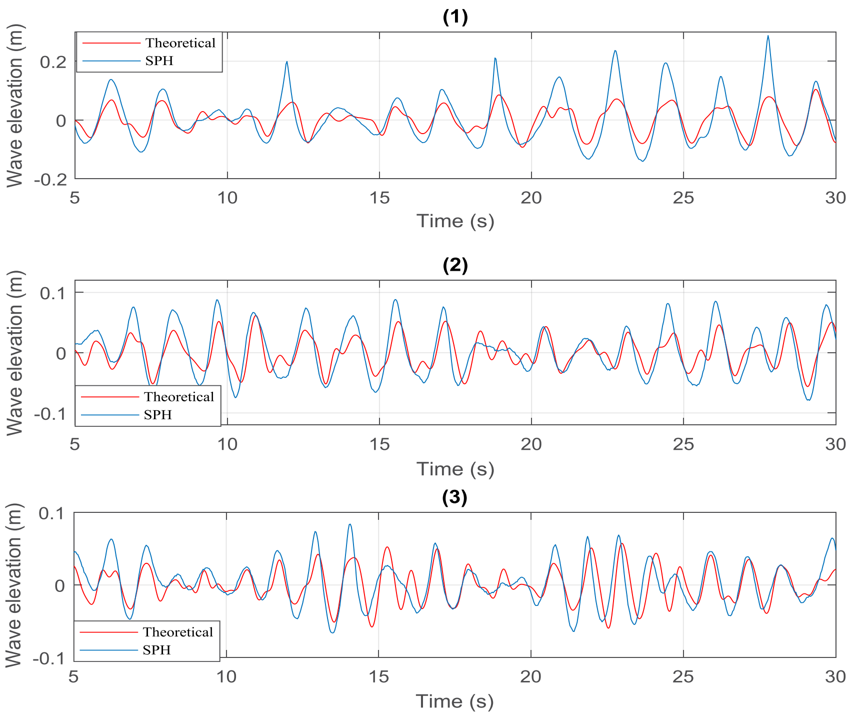

Figure 2: Comparison between theoretical and SPH wave amplitudes for JONSWAP wave spectrum test cases.

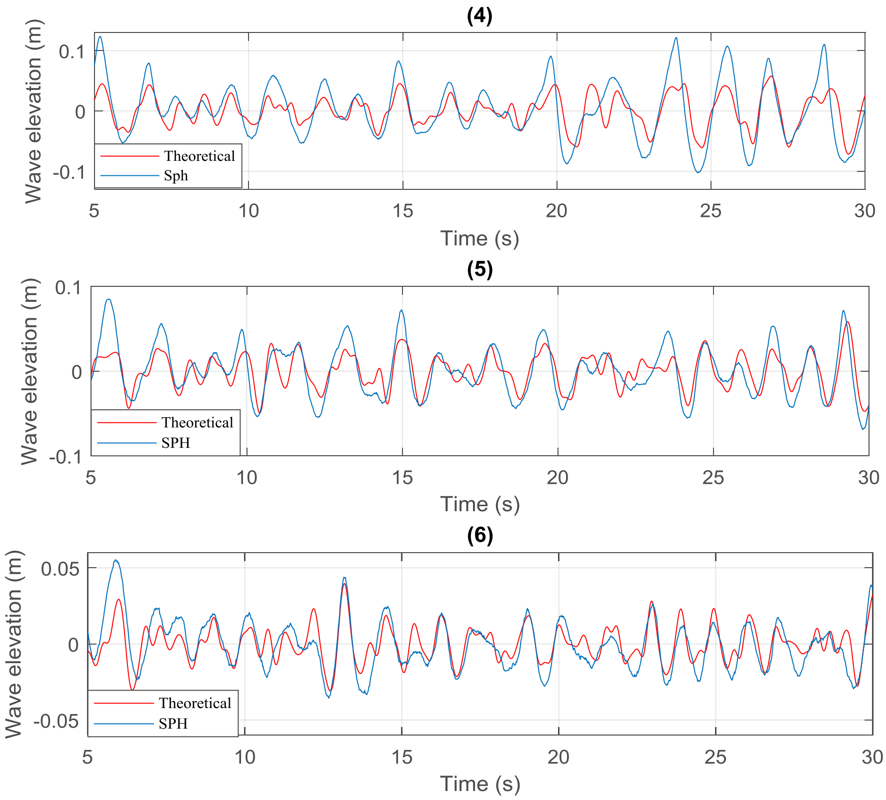

Figure 3: Comparison between theoretical and SPH numerical wave amplitudes for Pierson-Moskowitz wave spectrum test cases.

Fig.4 displays the wave energy spectrum of the SPH numerical results and expected theoretical energy density distribution for all test cases. In JONSWAP simulations, a reasonable agreement is achieved in terms of spectrum form, energy peak values, and the peak frequencies. As for the Pierson-Moskowitz wave spectrum simulations, the energy levels at higher frequency bands are consistent with the expected theoretical results however there occurs a wide peak-frequency zone in SPH results with high noise levels in energy results. The main source of the difference in energy levels of Pierson-Moskowitz simulations can arise due to the necessity of longer simulation times to mimic the fully developed and unlimited fetch sea conditions nature of the spectrum.

4 CONCLUDING REMARKS AND FUTURE WORK

This study aims to model a wave tank that can generate irregular waves which is highly required in research and development stages of many engineering fields such as shipbuilding, marine sciences, and coastal engineering. To provide a unique contribution to the solution of the engineering problems mentioned in this scope, the particle-based SPH algorithm is proposed together with the numerical correction treatments. The results obtained from the simulations compared with the theoretically calculated wave characteristics and energy densities. In the shed of the simulation results, it can be stated that quite promising agreement is achieved with the theoretical results in terms of wave characteristics and wave energy densities while long-term simulations for the Pierson-Moskowitz wave spectrum is still required to represent the whole characteristics of the wave train. As a concluding remark one can argue that the presented SPH-based numerical solution scheme can be assumed as a practical tool to investigate the problems regarding irregular wave generation systems.

In the next steps of this study, a piston-type wave generator will be adopted into the computational domain for generating the regular and irregular wave spectrums. As benchmark studies, JONSWAP and Pierson-Moskowitz wave spectrums will be simulated to validate the obtained wave characteristics with the theoretical results. Finally, a more challenging problem, namely, the dynamic behaviors of floating bodies under the effect of generated random waves will be investigated.

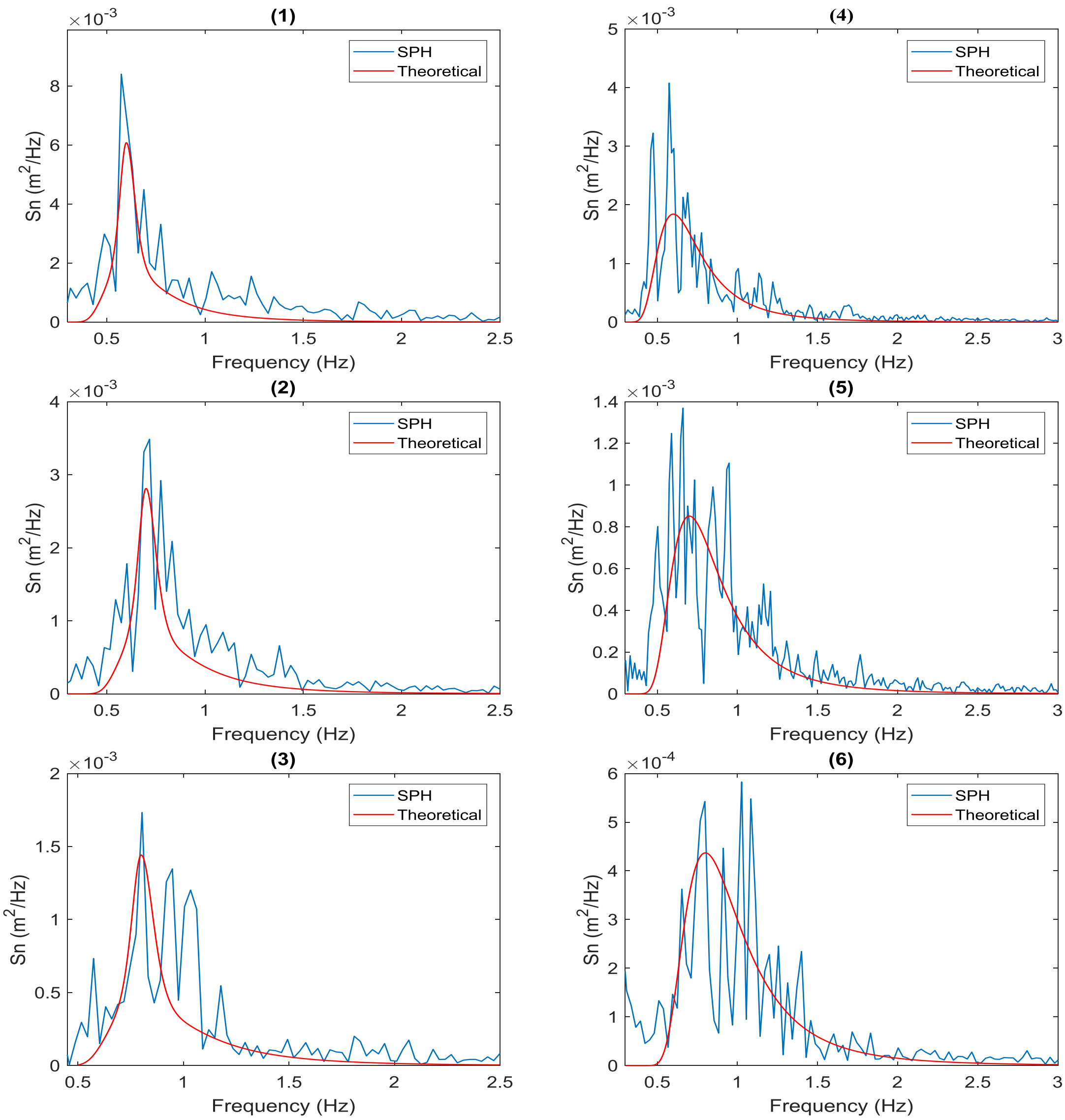

Figure 4: Comparison of theoretical and numerical spectral density for irregular waves.

5 ACKNOWLEDGEMENT

The authors gratefully acknowledge financial support provided by the Scientific and Technological Research Council of Turkey (TUBITAK) for project number 117M091.

REFERENCES

[1] Pierson, W. and M. St Denis, *On the motion of ships in confused seas.* Transactions SNAME, 1953. **61**: p. 280-354.

[2] Stansberg, C., et al., *The specialist committee on waves final report and recommendations to the 23rd ITTC.* Proceedings of the 23rd ITTC, 2002. **2**: p. 505-551.

[3] Hasselmann, K., et al., *Measurements of wind-wave growth and swell decay during the Joint North Sea Wave Project (JONSWAP).* Ergänzungsheft 8-12, 1973.

[4] Pierson Jr., W.J. and L. Moskowitz, *A proposed spectral form for fully developed wind seas based on the similarity theory of S. A. Kitaigorodskii.* Journal of Geophysical Research (1896-1977), 1964. **69**(24): p. 5181-5190.

[5] Boccotti, P., et al., *Field experiment on random wave forces acting on vertical cylinders.* Probabilistic Engineering Mechanics, 2012. **28**: p. 39-51.

[6] Boo, S., *Measurements of higher harmonic wave forces on a vertical truncated circular cylinder.* Ocean engineering, 2006. **33**(2): p. 219-233.

[7] Kim, C. and Z. Wangv, *Horizontal force of vertical truncated column in Stokes 5th-order waves.* International Journal of Offshore and Polar Engineering, 1999. **9**(03).

[8] Monaghan, J.J., *Simulating free surface flows with SPH.* Journal of computational physics, 1994. **110**(2): p. 399-406.

[9] Barreiro, A., et al., *Smoothed particle hydrodynamics for coastal engineering problems.* Computers & Structures, 2013. **120**: p. 96-106.

[10] Vanneste, D.F., et al., *Comparison of numerical models for wave overtopping and impact on a sea wall.* Coastal Engineering Proceedings, 2014. **1**(34): p. 5.

[11] Shadloo, M.S., et al., *Numerical simulation of long wave runup for breaking and nonbreaking waves.* International Journal of Offshore and Polar Engineering, 2015. **25**(01): p. 1-7.

[12] Liu, X., P. Lin, and S. Shao, *ISPH wave simulation by using an internal wave maker.* Coastal Engineering, 2015. **95**: p. 160-170.

[13] Altomare, C., et al., *Applicability of smoothed particle hydrodynamics for estimation of sea wave impact on coastal structures.* Coastal Engineering, 2015. **96**: p. 1-12.

[14] Monaghan, J. and A. Kos, *Solitary waves on a Cretan beach.* Journal of waterway, port, coastal, and ocean engineering, 1999. **125**(3): p. 145-155.

[15] Liu, G.-R., *Meshfree methods: moving beyond the finite element method*. 2009: CRC press.

[16] Müller, M., D. Charypar, and M. Gross. *Particle-based fluid simulation for interactive applications*. in *Proceedings of the 2003 ACM SIGGRAPH/Eurographics symposium on Computer animation*. 2003. Eurographics Association.

[17] Liu, M. and G. Liu, *Smoothed particle hydrodynamics (SPH): an overview and recent developments.* Archives of computational methods in engineering, 2010. **17**(1): p. 25-76.

[18] Monaghan, J.J., *Smoothed particle hydrodynamics.* Reports on progress in physics, 2005. **68**(8): p. 1703.

[19] Antuono, M., A. Colagrossi, and S. Marrone, *Numerical diffusive terms in weakly-compressible SPH schemes.* Computer Physics Communications, 2012. **183**(12): p. 2570-2580.

[20] Randles, P. and L. Libersky, *Smoothed particle hydrodynamics: some recent improvements and applications.* Computer methods in applied mechanics and engineering, 1996. **139**(1-4): p. 375-408.

[21] Khayyer, A., H. Gotoh, and S. Shao, *Corrected incompressible SPH method for accurate water-surface tracking in breaking waves.* Coastal Engineering, 2008. **55**(3): p. 236-250.

[22] Ozbulut, M., et al., *Investigation of wave characteristics in oscillatory motion of partially filled rectangular tanks.* Journal of Fluids Engineering, 2018. **140**(4): p. 041204.

[23] Meringolo, D.D., F. Aristodemo, and P. Veltri, *SPH numerical modeling of wave–perforated breakwater interaction.* Coastal Engineering, 2015. **101**: p. 48-68.

[24] Ozbulut, M., M. Yildiz, and O. Goren, *A numerical investigation into the correction algorithms for SPH method in modeling violent free surface flows.* International Journal of Mechanical Sciences, 2014. **79**: p. 56-65.

[25] Liu, Z. and P. Frigaard, *Generation and analysis of random waves.* 1999.

[26] Dean, R.G. and R.A. Dalrymple, *Water wave mechanics for engineers and scientists*. Vol. 2. 1991: World Scientific Publishing Company.